Available online at www.sciencedirect.com
ScienceDirect
Optik 121 (2010) 1330–1336
Optik Optics
www.elsevier.de/ijleo

Theoretical study of implementing an all-optical analogue-to-digital conversion based on the Mach–Zehnder interferometric configurations

Alexandre S. Shcherbakov, Ivan Hernandez Romano*

Department of Optics, National Institute for Astrophysics, Optics, and Electronics (INAOE), A.P. 51 and 216, Puebla, Pue. 72000, Mexico

Received 17 September 2008; accepted 10 January 2009

Abstract

A new technique of ultrafast analogue-to-digital (A-D) conversion for an all-optical data processing is proposed. This technique is based on the Kerr nonlinearity-induced cross-phase modulation in single-mode Mach–Zehnder interferometer configurations arranged in a specific way. Two schemes, capable of realizing both sequential and parallel A-D conversions of optical signals are considered. The potential for an extremely high-bit-rate processing, up to 1 THz in each converter, is due to a femtosecond time response of Kerr effect in fused silica glass. Optical schemes of proposed devices are presented and algorithmically estimated; their functional capabilities are discussed.

Keywords: Analogue-to-digital (A-D) converter; Self-phase modulation (SPM); Cross-phase modulation (CPM); Mach–Zehnder interferometric configuration

1. Introduction

Modern communication systems require high sampling rate analog-to-digital (A-D) converters. The electronic A-D converters with a speed of a few tens giga samples per second are reported by Nosaka et al. [1], but it is difficult to reach higher speed because their sample rate is limited by a number of mechanisms including thermal noise, sampling aperture jitter, and comparator ambiguity [2]. Optical devices have been implemented in the A-D converters to improve the performance of the sampling rate and quantization [3,4].

Ultrafast optical phenomena have been implemented to realize all-optical A-D conversion because they can get sampling rates higher than electronic A-D converters. All-optical devices exploiting nonlinear phase shifts induced in interferometers seem to be the most appropriate for optical computing systems due to their low energy consumption, rather simple schematic realization, ability to exploit the soliton propagation regime, high sensitivity to controlling pulses actuation along with possibility of internal transfer function realization. Recently, the nonlinear optical phenomena that have been used to produce A-D converters are: self-phase modulation (SPM) [5], four-wave mixing [6], generation of supercontinuum [7], and soliton self-frequency shifting [8]. Another A-D converter which is based on Sagnac interferometer has also been used [9]. The comprehensive review of A-D converters can be

*Corresponding author. Tel./fax: +52 222 2472940.
E-mail addresses: alex@inaoep.mx (A.S. Shcherbakov), hromano@inaoep.mx (I.H. Romano).

0030-4026/$ - see front matter © 2009 Elsevier GmbH. All rights reserved.
doi:10.1016/j.ijleo.2009.01.006

found in extensive review of Valley [10]. Evidently, one of the fastest nonlinearity in condensed-matter material is associated with the Kerr effect in fused silica glass, its response time is about a few femtoseconds.

In this work we propose a new all-optical technique of A-D conversion based on the Kerr nonlinearity-induced cross-phase modulation (CPM) in single-mode Mach–-Zehnder interferometer configurations.

2. Preliminary survey

Let us start from the consideration of a beam splitter presented by a partially silvered mirror or a single-mode fiber X-coupler, see Fig. 1. It is well known that a partially silvered mirror, depicted in Fig. 1a, reflects one portion of the light incident on it and refracts the other portion through it. The speed of light in air is almost the speed of light c in vacuum. In terms of the refractive index $n = c/v$, where v is the speed of light in a medium, the refractive index of air is almost exactly unity. The speed of light in glass is significantly less than c; for most glasses, the refractive index is close to 1.5 or so. In another words, the speed of light in glass is in the order of two-thirds of the speed of light in vacuum. When a light ray is incident on a surface and the material on the other side of the surface has a higher refractive index, the reflected light ray shifts its phase by exactly one half a wavelength. If a light ray is incident on a surface and the material on the other side of this surface has a lower refractive index, the reflected light ray does not have its phase changed. When a light ray goes from one medium into another, its direction changes due to refraction but no phase change occurs at the surface of these two media. Similar consideration can be explained relative to a single-mode fiber X-coupler, see Fig. 1b, if we take into account the phase shift of exactly half a wavelength needed to provide the mode coupling of two neighboring cores in the fiber coupler. Hence the electric fields at the outputs of beam splitter with the power splitting ratio α:(1−α) are given by [11]

$$\text{(a)}\quad E_3 = \sqrt{\alpha}E_1 + i\sqrt{1-\alpha}E_2, \quad \text{(b)}\quad E_4 = i\sqrt{1-\alpha}E_1 + \sqrt{\alpha}E_2, \tag{1}$$

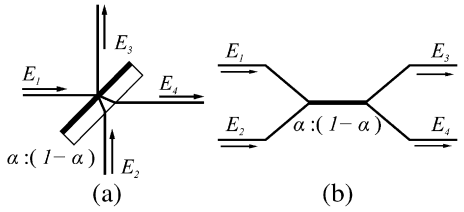

Fig. 1. Two possible beam-splitter devices: (a) partially silvered mirror and (b) single-mode fiber X coupler.

where $E_{1,2} = A_{1,2}\exp(i\Phi_{1,2})$; $A_{1,2}$ and $\Phi_{1,2}$ are the amplitudes and phases of the incident light waves. Eqs. (1) lead to the conservation law $|E_1|^2 + |E_2|^2 = |E_3|^2 + |E_4|^2 = A_1^2 + A_2^2$.

Then, Eqs. (1) can be exploited to analyze the looped fiber 3 dB X-coupler (i.e. with $\alpha = 1/2$) when one of the output ports is connected with one of the input ports, see Fig. 2a. Let us assume that the field A_2 is applied at the bottom left hand side port and represents just one incoming rectangular pulse of unit amplitude, whose spatial length is much shorter than an upper fiber loop length. Furthermore, the upper fiber loop length is shorter than the dispersion and nonlinear length scales associated with an optical pulse; they are 50 and 333.3 m, respectively (for standard telecommunication fibers at 1550 nm, 1 W of power and 1 ps of width). In this case, one can consider circulating such a pulse through a loop and shaping a train of the output pulses with the decreasing intensity, issuing from the bottom right hand side port. Details of the phase relations are not significant here due to linear approximation of this analysis. The first path through the X-coupler is characterized by the following amplitudes: $E_1 = 0$, $E_2 = A_2 = 1$, $E_3 = i/\sqrt{2}$, and $E_4 = 1/\sqrt{2}$, so that $|E_4|^2 = 1/2$. The second path gives $E_1 = i/\sqrt{2}$, $E_2 = 0$, $E_3 = i/2$, and $E_4 = -i/2$ with $|E_4|^2 = 1/4$. Thus, one can see that such a dividing device shapes a train of the output optical pulses whose intensities are decreased by a factor of two after each next circulation through a fiber loop. Consequently, this fiber scheme serves as a sequential intensity divider. Similar consideration can be carried out for a parallel intensity divider shown in Fig. 2b.

Now, one can consider the scheme of Mach–Zehnder configuration shown in Fig. 3. It consists of two arms providing the phase shifts $\phi_{1,2}$ and two beam splitters (or X-couplers in fiber arrangement) with the power splitting ratios α:(1−α) and β:(1−β), respectively. In this case, one can write

$$\text{(a)}\quad E_5 = E_3\exp(i\phi_1), \quad (b)\quad E_6 = E_4\exp(i\phi_2). \tag{2}$$

Then, using Eqs. (1), the electric fields at the output of Mach–Zehnder interferometer can be found:

$$\text{(a)}\quad E_7 = \sqrt{\beta}E_5 + i\sqrt{1-\beta}E_6, \quad \text{(b)}\quad E_8 = i\sqrt{1-\beta}E_5 + \sqrt{\beta}E_6. \tag{3}$$

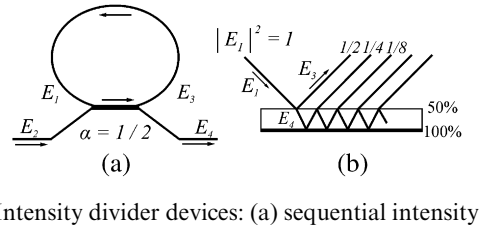

Fig. 2. Intensity divider devices: (a) sequential intensity divider based on fiber and (b) parallel intensity divider based on partial-silvered mirror.

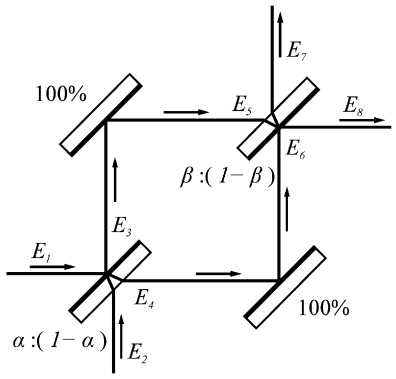

Fig. 3. Mach–Zehnder interferometeric configuration.

The complete expressions for the output light intensities with A_1, $A_2 \neq 0$ have the form

$$\begin{aligned}|E_7|^2 = {} & A_1^2\left[(\alpha-1)(\beta-1)+\alpha\beta-2\sqrt{\alpha-\alpha^2}\sqrt{\beta-\beta^2}\cos(\phi_1-\phi_2)\right] \\ & + A_2^2\left[\alpha+\beta-2\alpha\beta+2\sqrt{\alpha-\alpha^2}\sqrt{\beta-\beta^2}\cos(\phi_1-\phi_2)\right] \\ & + 2A_1A_2\Big\{\sin(\Phi_1-\Phi_2)\sqrt{\alpha-\alpha^2}(2\beta-1) \\ & + \sqrt{\beta-\beta^2}[\alpha\sin(\phi_1-\phi_2+\Phi_1-\Phi_2) \\ & + (1-\alpha)\sin(\phi_1-\phi_2-\Phi_1+\Phi_2)]\Big\}, \end{aligned} \tag{4}$$

$$\begin{aligned}|E_8|^2 = {} & A_1^2\left[\alpha+\beta-2\alpha\beta+2\sqrt{\alpha-\alpha^2}\sqrt{\beta-\beta^2}\cos(\phi_1-\phi_2)\right] \\ & + A_2^2\left[(\alpha-1)(\beta-1)+\alpha\beta-2\sqrt{\alpha-\alpha^2}\sqrt{\beta-\beta^2}\cos(\phi_1-\phi_2)\right] \\ & - 2A_1A_2\Big\{\sin(\Phi_1-\Phi_2)\sqrt{\alpha-\alpha^2}(2\beta-1) \\ & + \sqrt{\beta-\beta^2}[\alpha\sin(\phi_1-\phi_2+\Phi_1-\Phi_2) \\ & + (1-\alpha)\sin(\phi_1-\phi_2-\Phi_1+\Phi_2)]\Big\}, \end{aligned} \tag{5}$$

with $\alpha = \beta = 1/2$ and $\Phi = \Phi_1 - \Phi_2$, one can arrive at

$$\begin{aligned}|E_7|^2 = {} & \frac{A_1^2}{2}[1-\cos(\phi_1-\phi_2)] + \frac{A_2^2}{2}[1+\cos(\phi_1-\phi_2)] \\ & + A_1A_2\sin(\phi_1-\phi_2)\cos(\Phi), \end{aligned} \tag{6}$$

$$\begin{aligned}|E_8|^2 = {} & \frac{A_1^2}{2}[1+\cos(\phi_1-\phi_2)] + \frac{A_2^2}{2}[1-\cos(\phi_1-\phi_2)] \\ & - A_1A_2\sin(\phi_1-\phi_2)\cos(\Phi). \end{aligned} \tag{7}$$

3. Effects of the self- and cross-phase modulation in a low-loss medium

The Kerr nonlinearity in silica glass is a third-order effect, in which the refractive index n depends on the intensities of the light beams co-propagating along a medium as

$$n = n_0 + n_2 I + \tilde{n}_2 \tilde{I}, \tag{8}$$

where n_0 is the linear refractive index, n_2 is the nonlinear Kerr coefficient responsible for the self-action of the main light field with the intensity I, $\tilde{I}$ is an external light beam intensity (if it exists), $\tilde{n}_2$ is the Kerr coefficient describing a mutual influence of the light fields I and $\tilde{I}$; $\tilde{n}_2 = 2n_2/3$, when the polarization state of the light field I is orthogonal to the polarization of the field $\tilde{I}$, and $\tilde{n}_2 = 2n_2$ for the same polarization states of these fields [12]. To take into account the linear optical losses in a medium one can introduce the factor Γ, characterizing the losses per unit length. Assuming that the pulse width is short compared with the arm length L, the nonlinear phase shift φ acquired by the propagating light field of the wavelength λ under the influence of the self-phase modulation in a low-loss medium can be described by

$$\text{(a)}\quad \varphi = 2\pi\lambda^{-1}n_2 I L_0, \quad \text{(b)}\quad L_0 = \Gamma^{-1}[1-\exp(\Gamma L)], \tag{9}$$

where L_0 is the effective length of propagation caused by the linear optical losses.

Providing a mutual influence of the light fields I and $\tilde{I}$, the cross-phase modulation takes place. The nonlinear phase shift ψ in the field I acquired by the co-propagating light field $\tilde{I}$ of the wavelength $\tilde{\lambda}$ due to the CPM effect can be estimated by

$$\psi = 2\pi\tilde{\lambda}^{-1}\tilde{n}_2\tilde{I}L_0. \tag{10}$$

It follows from Eq. (8) that the effects of self- and cross-phase modulation are additive in behavior. Additionally, the influence of linear optical losses should be included in Eqs. (4)–(7) through multiplying by the term $\exp(-\Gamma L)$. In particular, Eqs. (6) and (7) have to be rewritten for a low-loss medium as

$$\begin{aligned}|E_7|^2 = {} & \Big\{\frac{A_1^2}{2}[1-\cos(\phi_1-\phi_2)] + \frac{A_2^2}{2}[1+\cos(\phi_1-\phi_2)] \\ & + A_1A_2\sin(\phi_1-\phi_2)\cos(\Phi)\Big\}\exp(-\Gamma L), \end{aligned} \tag{11}$$

$$\begin{aligned}|E_8|^2 = {} & \Big\{\frac{A_1^2}{2}[1+\cos(\phi_1-\phi_2)] + \frac{A_2^2}{2}[1-\cos(\phi_1-\phi_2)] \\ & - A_1A_2\sin(\phi_1-\phi_2)\cos(\Phi)\Big\}\exp(-\Gamma L). \end{aligned} \tag{12}$$

4. All-optical switching in the nonlinear Mach–Zehnder configuration

Let us consider exploiting the nonlinear Mach–Zehnder interferometer with $\alpha = \beta = 1/2$ and choose now a

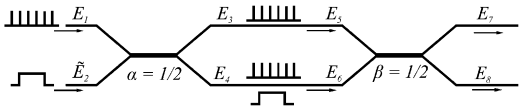

Fig. 4. Nonlinear Mach–Zehnder fiber interferometric configuration.

fiber arrangement of the interferometer. One can provide such a regime that the field E_1 represents a train of short optical pulses, while the field $\tilde{E}_2$ includes only one relatively long optical pulse with an ideal rectangular shape of envelope, see Fig. 4. The fields E_1 and $\tilde{E}_2$ should not interfere with each other due to the difference, for example, in their wavelengths (λ and $\tilde{\lambda}$, respectively) or in their polarization states. Moreover, we assume that the interferometer includes the selective input X-coupler (or beam splitter in the bulk arrangement), which is arranged so that the field E_1 of short pulses is equally divided between two arms using the input splitter, while the field $\tilde{E}_2$ of a long pulse enters only one of the arms. Similar separation of light fields can be achieved using either spectral or polarization selectivity of the input coupler (beam splitter).

In this case, the light intensities at the output ports are caused by an interference between two portions of the field E_1 and governed by Eqs. (11) and (12) with $A_1^2 = |E_1|^2$ and $A_2 = 0$. The chosen regime leads to the nonlinear phase shift $\phi_1 = \varphi_1 = \pi\lambda^{-1} n_2 A_1^2 L_0$ because of the SPM effect in an upper arm of fiber Mach–Zehnder interferometer and to the nonlinear phase shift $\phi_2 = \varphi_1 + \psi_2 = \pi\lambda^{-1} n_2 A_1^2 L_0 + 2\pi\tilde{\lambda}^{-1}\tilde{n}_2|\tilde{E}_2|^2 L_0$ due to the additive contributions of both the SPM and the CPM effects in the bottom arm. As a result, one can easily estimate the combined nonlinear phase shift as

$$\phi_1 - \phi_2 = -2\pi\tilde{\lambda}^{-1}\tilde{n}_2\left|\tilde{E}_2\right|^2 L_0. \tag{13}$$

Let us assume now that $-2\pi\tilde{\lambda}^{-1}\tilde{n}_2|\tilde{E}_2|^2 L_0 = (2k+1)\pi$, where k is a whole number, positive or negative. In the last case, one can obtain from Eqs. (11) and (12) that

$$|E_7|^2 = 0, \quad |E_8|^2 = A_1^2 \exp(-\Gamma L), \quad \text{with} \quad \tilde{E}_2 = 0, \tag{14}$$

or

$$|E_7|^2 = A_1^2 \exp(-\Gamma L), \quad |E_8|^2 = 0, \quad \text{with} \quad \tilde{E}_2 \neq 0. \tag{15}$$

Consequently, the selected regime provides an all-optical switching for the desirable fraction of a short optical pulse train from one input port to one of the two output ports. In so doing, the other rather long optical pulse, applied to the second input port, plays a role of the controlling pulse. In fact, by this it means that the nonlinear Mach–Zehnder interferometer performs demultiplexing the input optical pulse train, which could present a binary-encoded optical data stream.

5. Sequential analogue-to-digital conversion in the nonlinear Mach–Zehnder fiber interferometric configuration

Here, we propose a new principle of the analogue-to-digital conversion based on the CPM effect in the nonlinear Mach–Zehnder fiber interferometric configuration. The sequential scheme of an all-fiber A-D converter is presented in Fig. 5. It consists of the looped fiber 3 dB X-coupler (see Section 2), the nonlinear Mach–Zehnder fiber interferometer (see an analogue in Section 4) with an additional phase-shifting component, and the threshold device. The divided parts of an original analogue signal I_S with the intensities I_S^* (here, $I_S^* = \{I_S/2, I_S/4, I_S/8, \ldots\}$) are applied at one input port of the interferometer. A selective input X-coupler directs them into a bottom arm only. The sampling pulses of the reading beam are applied at the other input port, divided into a pair of equal portions by that input X-coupler, and distributed into both the arms. These two portions of the reading pulses with the same intensities I_R and the signals with the intensities I_S^* propagate through the interferometer arms simultaneously, so that the signal fields affect only one of the reading beam portions. Then, two portions of the reading pulses interfere in the selective output 3 dB X-coupler, which barred of the signal beam. Finally, one of the output fractions, being a result of interference, reaches the threshold device.

Thus, the output intensity is given by Eq. (11) with $A_1 = 0$ and $A_2 = \sqrt{2I_R}$, i.e.

$$|E_7|^2 = I_R[1 + \cos(\phi_1 - \phi_2)]\exp(-\Gamma L). \tag{16}$$

The combined phase shifts can be estimates as

$$\begin{aligned} &\text{(a)} \quad \phi_1 = 2\pi\lambda_R^{-1} n_2 I_R L_0 + \theta, \\ &\text{(b)} \quad \phi_2 = 2\pi\lambda_R^{-1} n_2 I_R L_0 + 2\pi\lambda_S^{-1}\tilde{n}_2 I_S^* L_0, \end{aligned} \tag{17}$$

where θ is the initial phase shift regulated, for example, by the piezoceramic cylinder. The second term in Eq. (17b) describes the nonlinear phase shift acquired by the reading beam of the wavelength λ_R due to the

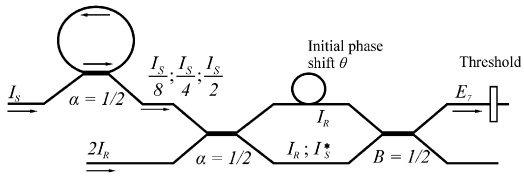

Fig. 5. Sequential scheme of an all-fiber A-D converter.

CPM influence of the signal beam. Consequently,

$$\phi_1 - \phi_2 = \theta - 2\pi\lambda_S^{-1}\tilde{n}_2 I_S^* L_0. \quad (18)$$

One can see from Eqs. (16) and (18) that one can obtain a periodic dependence for the output light intensity upon analogue values of I_S^* at the sample times of the reading pulses. Therefore, one can use the fundamental principle of A-D conversion, which proclaims the homomorphism between periodic change of the binary representation of analogue quantity and periodic output–input characteristic of the employed device [9]. Usually, a set of periodic characteristics with the periods being multiple of two has to be produced with a threshold at their outputs.

There are four possible versions of such a set with various initial phase shifts $\theta = \{0, \pi/2, \pi, 3\pi/2\}$. Each set forms a binary code definitely related to the original output. The set for conversion into the direct binary code is shown in Fig. 6, where figures from (a)–(c) refer to more significant bits. Thresholding at a level of 1/2 is depicted as the solid line characteristics along with ideal sinusoidal characteristics. One can see that each value of the input signal corresponds to the digital binary code. Note that increase and decrease of the curves at the 1/2 level should refer to the 1 and 0 output levels, respectively. Otherwise, the input value can be established as $1+\Delta$ with $\Delta < N^{-1}$, where N is the number of bits inherent in the A-D converter.

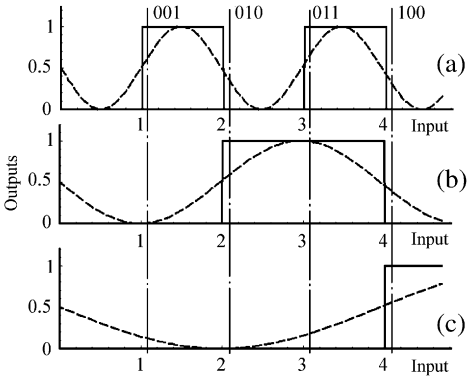

Fig. 6. Transfer functions and corresponding quantization rule (a), (b), and (c).

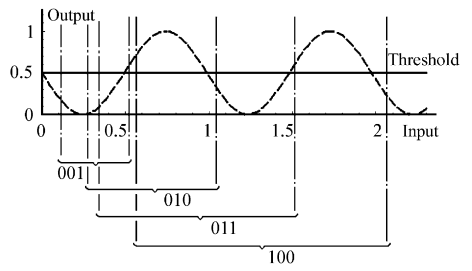

Fig. 7. Conversion of analog input into binary code.

For our purposes, the input signal can be preliminarily divided by a factor of two and a single nonlinear element having periodic output–input characteristics can be exploited. With the proper initial phase shift θ and a 1/2 level of thresholding, the curve in Fig. 7 makes available conversion into the direct binary code as in the case of a set of the curves in Fig. 6. The period of this characteristic is one half of the least significant bit (LSB) characteristic period, see Fig. 6a. It is seen from Fig. 7 that the set of 1/2, 1/4, 1/8, etc. fractions of an original input signal, being applied as the input signals, produce the same output bits as the set of characteristics with different periods in Fig. 6, i.e. A-D conversion of the input signal takes place.

The transfer function of the nonlinear interferometer described by Eqs. (16) and (18) is evidently similar to the curve in Fig. 7 with $\theta = \pi/2$, a threshold level of $I_R \exp(-\Gamma L)$, and an intensity increment in the input signal beam, which causes one period variation at the output, being taken as the unit intensity. In our scheme, see Fig. 5, the dividing device with the intensity decreasing ratio of two is formed by the looped fiber 3 dB X-coupler, while the needed initial phase shift is produced by the piezoelectric cylinder. Therefore, the configuration in Fig. 5 represents an all-optical fiber A-D converter. The first pulse referring to the intensity $I_S/2$ generates the least significant bit, and the last pulse matching the intensity of $2^{-N}I_S$, which is greater than a half of the unit intensity, lets out the most significant bit (MSB).

6. Parallel analogue-to-digital conversion in the bulk interferometric configuration

Fig. 8 shows the parallel version of the A-D converter. An original analogue signal with the intensity I_S is now divided into a space beamlet set with the intensities I_S^* (where again $I_S^* = I_S/2, I_S/4, I_S/8, \ldots$) due to multiple reflections in the dividing plate (see Section 2) having one half-transparent and one completely reflecting surfaces. The dividing plate forms a set of signal beams. An analog signal and a set of ultrashort sampling optical pulses of the reading beams coincide on the left hand

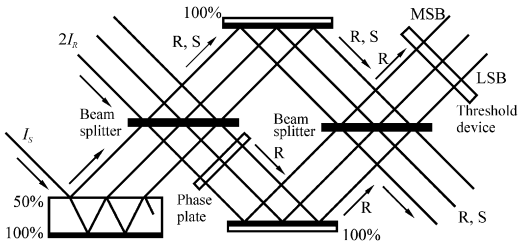

Fig. 8. Parallel version of the A-D converter based on partially silvered mirrors and beam splitters.

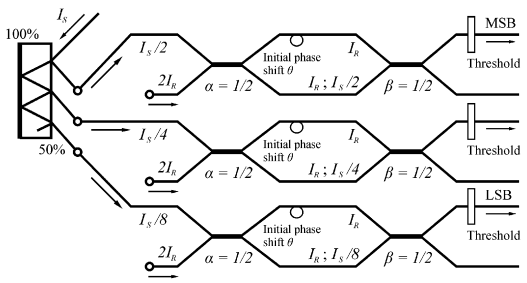

Fig. 9. Parallel all-optical A-D converter based on nonlinear Mach–Zehnder fiber interferometric configuration.

side beam splitter, which is a 3 dB optical splitter for the reading beams and completely transparent for the signal beams. The right hand side beam splitter has the same properties and functional capabilities as the left one. These components can be fabricated using a half-transparent mirror and polarizer or on the base of the polarizing prisms. The phase plate produces a linear phase shift allowing the conversion into the standard binary presentation, see Figs. 6 and 7. An intensity increment in the input signal beam, which causes a one period variation at the output port, is taken as the unit intensity. With proper threshold, the output signal is the binary digits representing the intensity of the input signal. The first beamlet generates the most significant bit. The final beamlet, whose intensity is greater than a half of the unit intensity, gives the least significant bit. As the threshold, a bistable device, which operates by controlling light with light, may be exploited [13].

The most important disadvantage inherent in the parallel A-D converter from Fig. 8 caused by the necessity of creating (exploiting, producing) a rather large volume of optically nonlinear material. Such a difficulty suggests that the schemes from Figs. 5 and 8 can be combined, as it is shown in Fig. 9, to design another version of the parallel all-optical A-D converter.

7. Numerical estimations

The necessary splitting ratios for signal and reading beams (see Sections 5 and 6) can be realized using spectral or/and polarization selectivity of beam splitters. In both the cases, the difference Δn of refractive indices causes complete time mismatch between the signal and the reading optical pulses with the duration τ along the propagation length

$$L_{\max} = (\Delta n)^{-1} c\tau. \tag{19}$$

Since one needs a value of $2\pi\lambda_S^{-1}\tilde{n}_2 I_S^* L_0 = 2\pi$ in Eq. (18) for unit level if the signal intensity, minimal energy density of the optical signal can be estimated by

$$\frac{\mathscr{E}_{\min}}{S} = \frac{\lambda_S \Delta n}{c\tilde{n}_2}, \tag{20}$$

where S an effective cross-section of the beam or the fiber core; $\tilde{n}_2 = 2n_2/3$ for orthogonal states of polarization and $n_2 \approx 3.2 \times 10^{-16}\,\mathrm{cm^2/W}$ for fused silica glass. Let us assume that $\Delta n = 10^{-4}$, which is typical, for example, for polarization preserving fibers [14], $\lambda_S = 1550\,\mathrm{nm}$, and $\tau = 1\,\mathrm{ps}$, so that one can obtain $L_{\max} = 3\,\mathrm{m}$ and $\mathscr{E}_{\min}/S = 24\,\mathrm{pJ/\mu m^2}$.

For weak signals, the value of $L_{\max}$ should be increased. It can be realized using different wavelengths of the orthogonally polarized light fields to compensate Δn. For instance, the difference $\Delta n = 10^{-4}$ at a wavelength of 1550 nm can be compensated by the wavelength shift of about 10 nm. In that case, the main restricting factor is conditioned by the linear optical losses in a medium, which reduce the effective length L_0 of pulse propagation. For example, when losses are equal to 0.4 dB/km, i.e. $\Gamma = 0.092\,\mathrm{km^{-1}}$, one can estimate that $L_0 \leqslant 11\,\mathrm{km}$. Thus, the minimal energy density, which we indicated by suffix "1", is given by

$$\frac{\mathscr{E}_1}{S} = \frac{\lambda_S \tau}{\tilde{n}_2 L_0}, \tag{21}$$

which leads for $\tau = 1\,\mathrm{ps}$ and $L_0 = 10\,\mathrm{km}$ to $\mathscr{E}_{\min}/S = 7 \times 10^{-3}\,\mathrm{pJ/\mu m^2}$. The energy density range of N-bit converter can be estimated as

$$\frac{\mathscr{E}_1}{S} < \frac{\mathscr{E}}{S} < (2^N - 1)\frac{\mathscr{E}_1}{S}. \tag{22}$$

With $N = 10$, one can obtain $(2^N - 1)(\mathscr{E}_1/S) \approx 7\,\mathrm{pJ/\mu m^2}$.

8. Conclusion

We have presented the general consideration of applying the nonlinear Mach–Zehnder interferometric configurations for an all-optical A-D conversion. The concept, taking into account influence of the CPM effect on high-bit-rate data flows, has been developed. The schemes of new all-optical A-D converters, sequential and parallel, have been presented. The effects of self- and cross-phase modulation effects due to the Kerr nonlinearity are fundamental for providing time performances of schemes under analysis and make it possible to design ultrafast converters for high-bit-rate optical processing. Principles of operation and functional capabilities of novel A-D converters are described and discussed.

For practical realization of the A-D converter under proposal, one can meet several difficulties such thresholding with proper speed of operation, the problem of instability in the Mach–Zehnder interferometer, and fabrication of X-coupler with required splitting properties. We suppose that electro-optical A-D converters are preferably suitable for the sampling frequencies less than 10 GHz. However, only all-optical schemes using

extremely fast responsive phenomena, for instance Kerr nonlinearity in silica glass, can provide the sampling frequencies up to 1 THz.

Acknowledgment

This work was financially supported by CONACyT, Mexico, Project # 61237.

References

[1] H. Nosaka, M. Nakamura, M. Ida, K. Kurishima, T. Shibata, M. Muraguchi, A 24-Gsps 3-bit Nyquist ADC using InP HBTs for electronic dispersion compensation, in: Proceedings of the International Microwave Symposium, vol. 1, 2004, pp. 101–104.
[2] R.H. Walden, Analog-to-digital converter survey and analysis, IEEE J. Sel. Areas Commun. 17 (4) (1999) 539–550.
[3] K. Ma, R. Urata, D.A.B. Miller, J.S. Harris Jr., Low-temperature growth of GaAs on Si used for ultrafast photoconductive switches, IEEE J. Quantum Electron. 40 (6) (2004) 800–804.
[4] R.F. Pease, K. Ioakeimidi, R. Aldana, R. Leheny, Photoelectronic analog-to-digital conversion using miniature electron optics: basic design considerations, J. Vac. Sci. Technol. 21 (6) (2003) 2826–2829.
[5] T. Konishi, K. Tanimura, K. Asano, Y. Oshita, Y. Ichioka, All-optical analog-to-digital converter by use of self-frequency shifting in fiber and a pulse-shaping technique, J. Opt. Soc. Am. B 19 (11) (2002) 2817–2823.
[6] S. Oda, A. Maruta, K. Kitayama, All-optical quantization scheme based on fiber nonlinearity, IEEE Photonic Technol. Lett. 16 (2) (2004) 587–589.
[7] S. Oda, A. Maruta, A novel quantization scheme by slicing supercontinuum spectrum for all-optical analog-to-digital conversion, IEEE Photonic Technol. Lett. 17 (2) (2005) 465–467.
[8] C. Xu, X. Liu, Photonic analog-to-digital converter using soliton self-frequency shift and interleaving spectral filters, Opt. Lett. 28 (12) (2003) 986–988.
[9] K. Ikeda, J.M. Abdul, S. Namiki, K. Kitayama, Optical quantizing and coding for ultrafast A/D conversion using nonlinear fiber-optic switches based on Sagnac interferometer, Opt. Express 13 (11) (2005) 4296–4302.
[10] G.C. Valley, Photonic analog-to-digital converters, Opt. Express 15 (5) (2007) 1955–1982.
[11] J.E. Heebner, V.W. Wong, A. Schweinsberg, R.W. Boyd, D.J. Jackson, Optical transmission characteristics of fiber ring resonators, IEEE J. Quantum Electron. 40 (6) (2004) 726–730.
[12] G.P. Agrawal, Nonlinear Fiber Optics, third ed., Academic Press, San Diego, 2001.
[13] R.W. Boyd, Nonlinear Optics, second ed., Academic Press, New York, 2003.
[14] G.P. Agrawal, Fiber-Optics Communication Systems, third ed., Wiley, New York, 2002.